

# Supersolid Stripes Enhanced by Correlations in a Raman Spin-Orbit-Coupled System

J. Sánchez-Baena,<sup>1,\*</sup> J. Boronat,<sup>1,†</sup> and F. Mazzanti<sup>1,‡</sup>

<sup>1</sup>*Departament de Física, Universitat Politècnica de Catalunya,  
Campus Nord B4-B5, E-08034, Barcelona, Spain*

(Dated: January 20, 2020)

A Bose gas under the effect of Raman Spin-Orbit Coupling (SOC) is analyzed using the Discrete Spin T-moves Diffusion Monte Carlo method [1, 2]. By computing the energy as well as the static structure factor and the superfluid fraction of the system, the emergence of an energetically favorable supersolid stripe state is observed, which is in agreement with recent observations. A significant enhancement of the stability of the stripe phase with respect to the mean-field prediction is observed when the strength of the inter-atomic correlations is increased. We also quantify and characterize the degree of superfluidity of the stripes and show that this quantity is mostly determined by the ratio between the Raman coupling and the square of the momentum difference between the pair of SOC inducing laser beams.

Spin-Orbit Coupling (SOC), which denotes the interplay between a particle's momentum and its spin, has been a subject of interest in the recent years, both theoretically and experimentally. This is due to the wide variety of exotic quantum states induced by this kind of interaction, which include topological insulators [3], topological superconductors [4], and Majorana fermions [5]. SOC is a relativistic effect that emerges naturally in electronic systems, and that is also synthetically engineered [6] in ultracold atomic gases. These recent realizations in dilute gases represent an important achievement in the study of the physics of SOC due to the high controllability and tunability of these systems. In the particular case of Raman SOC, its implementation was first achieved experimentally by inducing a Raman coupling via two laser beams on an atomic Lambda type configuration. SOC is then generated by the simultaneous driving of a spin flip transition and transferring of momentum [7–11]. Under this scheme, Raman SOC has been realized with <sup>87</sup>Rb bosons, both in the continuum [7] and in a lattice [12, 13], and also with other species: <sup>6</sup>Li [14], <sup>40</sup>K [15], <sup>87</sup>Sr [16], <sup>173</sup>Yb [17, 18], and <sup>161</sup>Dy [19]. In this context, two hyperfine states of the atom are labeled as the spin states.

In this Letter, we focus in Raman SOC, which couples the linear momentum of an atom with its spin according to

$$\hat{W}^{\text{SOC}} = \frac{\hbar k_0}{m} \hat{P}_x \hat{\sigma}_z + \frac{\hbar^2 k_0^2}{2m} - \frac{\Omega}{2} \hat{\sigma}_x, \quad (1)$$

with  $m$  the mass of the particle,  $\hat{P}_x$  the  $x$ -component of the momentum,  $\hat{\sigma}_x$  and  $\hat{\sigma}_z$  the Pauli matrices,  $\Omega$  the Raman coupling, and  $k_0$  the magnitude of the wave vector difference between the two laser beams. Some striking features induced by the SOC interaction can be observed already at the single particle level. The coupling between momentum and spin implies that the minimum of the energy dispersion relation is in a non-zero momentum, degenerate state for a given range of values of the Raman coupling [20]. This degeneracy involves states of equal magnitude but opposite sign in momentum space,

enabling the possibility of a stripe phase ground state.

Supersolid stripes arise from the breaking of two symmetries: a gauge symmetry, giving rise to off-diagonal long-range order, and spatial symmetry, seen as a periodic density modulation in space [21]. The emergence and characterization of stripes in SOC systems have been a subject of major relevance in the field, both from the theoretical [21, 22] and experimental sides [23]. Despite being predicted by theory, the stripe phase was not detected in the first experimental realization of Raman SOC by Spielman's group [7], mainly due to the extremely low spin dependence of the inter-atomic interactions between <sup>87</sup>Rb atoms. Later on, stripes were observed by Ketterle's group [23] using a new Raman SOC setup with <sup>23</sup>Na that allowed for a better control of the spin interactions. Recently, they have also been detected in another experiment with <sup>87</sup>Rb atoms [24], where the contrast of the stripes is enhanced by rapidly increasing the Raman coupling before probing the density modulations by optical Bragg scattering.

In previous theoretical works, the phase diagram of an interacting system of atoms under Raman SOC has been reported [20, 25]. However, the diagram is restricted to the mean-field regime, valid only for very low gas parameter values,  $na^3 \leq \mathcal{O}(10^{-5})$ , with  $n$  and  $a$  the density and the s-wave scattering length, respectively. Moreover, although the superfluid character of the stripe phase has already been discussed [21, 22], a quantitative measure of the superfluid fraction is still missing, together with its characterization as a function of the different parameters of the problem. In order to address these issues and to deal with the non-local character of the SOC interaction, we use the Discrete Spin T-moves Diffusion Monte Carlo method (DTDMC) [1, 2, 26] to study the system from a microscopic point of view. Starting from a variational ansatz, we propagate the initial wave function in imaginary time keeping its phase constant, leading to a statistical representation of the best possible wave function given a phase constraint (fixed-phase approximation). DTDMC is then used to sample relevant ob-

servables, some of which may not be easily calculated at the mean-field level. An exact form of the imaginary time propagator up to first order in the time step is employed.

We study a three-dimensional system of  $N$  bosons of mass  $m$  under periodic boundary conditions (PBC) described by the Hamiltonian

$$\hat{H} = \sum_i \left[ \frac{\hat{P}_i^2}{2m} + \hat{W}_i^{\text{SOC}} \right] + \sum_{i<j} \hat{V}_{ij}, \quad (2)$$

where  $\hat{V}_{ij}$  is a short-range, two-body, spin-dependent interaction. We use two model interactions: a soft-sphere (SS) potential of strength  $V_0(s_i, s_j)$  and range  $R_0(s_i, s_j)$ , and a Lennard-Jones (LJ) force  $V_{ij}(r_{ij}, s_i, s_j) = \left( \frac{\sigma_{12}(s_i, s_j)}{r_{ij}} \right)^{12} - \left( \frac{\sigma_6(s_i, s_j)}{r_{ij}} \right)^6$ . Here,  $r_{ij}$  is the distance between the  $i$ -th and  $j$ -th particles and  $s_i, s_j = \pm 1$  are their spins. The trial wave function used for importance sampling in the DTDMC method, that also fixes the phase, is chosen as a product of one-body and two-body (Jastrow) terms. For the former, we use the expression reported in Ref. [20], with the sign of the spin-down component changed due to the different sign of the  $\Omega$  term in the Hamiltonian. The Jastrow factor depends on the interaction  $\hat{V}_{ij}$ . For the SS potentials we use the zero-energy solution of the averaged interaction along the different spin channels, which provides a lower variational energy than a spin-dependent two-body Jastrow factor. In the case of the LJ interaction a McMillan factor of the form  $e^{-(b/r)^5}$  is used, with  $b$  a constant that is variationally optimized. The choice of the parameters of the two-body interaction  $\hat{V}_{ij}$  determines the different channel scattering lengths  $a_{s,s'}$ , as according to Ref. [27] the inclusion or not of the SOC term does not appreciably change them. The values used in this work fulfill the condition  $a_{+1,+1} = a_{-1,-1} > a_{+1,-1} = a_{-1,+1}$ , as in the experiments of Ref. [23]. Finally, we express all quantities in dimensionless form, introducing characteristic length ( $a_0 = 1/k_0$ ) and energy ( $E_0 = \hbar^2 k_0^2 / 2m$ ) scales.

In order to characterize the phase diagram of the model, we use the standard gas parameter  $na^3$ , with  $a = a_{+1,+1}$  the scattering length of the interaction in the  $(+1, +1)$  channel. It should be noted that, for this system,  $na^3$  is not a scaling parameter. However, we use it to characterize the combined effect of the density and the interaction. We have checked, though, that for very low values of  $na^3$  one recovers the mean-field results, while for larger values, the DTDMC simulations reveal that the extension of the stripe phase domain is increased with respect to the mean-field prediction. This may be a relevant issue for experiments willing to detect and/or characterize the stripe phase. In order to illustrate that, we set the density to  $n = 3.7 \cdot 10^{-2}$ , with the number of particles  $N \in [50, 120]$  and the size of the simulation box changing as a function of the momentum of the trial wave function. We tune the spin-dependent scattering

lengths such that  $na^3 \in (10^{-4}, 10^{-1})$  by changing the two-body potential parameters. In this sense, increasing the gas parameter is equivalent to increasing the range and strength of the interactions, which enhances the effect of correlations in the medium. We set the interaction contrast  $\gamma = (a - a_{+1,-1}) / (a + a_{+1,-1})$  to  $\gamma = 0.4$ , since non-zero values of this quantity are necessary for the existence of a stripe ground state [20]. The quantitative characterization of the superfluidity in the stripe phase is performed with the contrast used in Ref. [23],  $\gamma = 0.904$ . It must be remarked that the quantity  $\gamma$  is a tunable property in the experimental setup of Ref. [23].

The phase diagram of the SOC system is reported in Fig. 1 for fixed density and varying scattering length. The upper and middle plots correspond to the DTDMC results for the SS and LJ interactions, respectively, while the lower plot shows the mean-field phase diagram. The points indicate the computed transition lines between the different phases. Errorbars in the DTDMC results account for the statistical variance of the energy estimations. Looking at the DTDMC phase diagrams it can be seen that, as the two-body scattering length increases, the value of the reduced Raman coupling at which the plane wave-stripe phase transition takes place, also increases. Remarkably, this effect is absent at the mean-field level, and is also robust with respect to the interaction employed. Based on this, we conclude that the enhancement of the stripe phase in the DTDMC phase diagrams is produced by the increase of inter-atomic correlations. This enhancement takes place because the DTDMC correction to the energy of the stripe ( $\Delta E_{\text{DMC,S}}$ ) and plane wave ( $\Delta E_{\text{DMC,PW}}$ ) phases and the energy difference between these phases at the mean-field level ( $\Delta E_{\text{MF}}$ ) fulfill  $\left| \frac{\Delta E_{\text{DMC,S}}}{\Delta E_{\text{MF}}} \right| \simeq \left| \frac{\Delta E_{\text{DMC,PW}}}{\Delta E_{\text{MF}}} \right| \simeq 1$  over a wide region of the phase diagram. The stripe phase is favoured over the plane wave phase in the DTDMC diagram because of the different polarization between phases: while the stripe phase is always unpolarized, the plane wave phase has non-zero polarization. Since the potentials employed in this work are less repulsive in the  $(+1, -1)$  and  $(-1, +1)$  channels in accordance to the experiment of Ref. [23], the beyond mean-field corrections favour an unpolarized state over a polarized one. In this sense, the DTDMC corrections drastically determine the transition line. In contrast, the single minimum region of the diagram is only slightly changed by DTDMC with respect to the mean-field prediction. This is because the energy gap in mean-field between this phase and the stripe and plane wave phases is larger in absolute value than the DTDMC corrections over the majority of the phase diagram.

In mean-field, the stripe-plane wave and the stripe-single minimum transitions are of first order, while the plane wave-single minimum transition is of second order [6, 25]. This is directly reflected in the value of the momentum that minimizes the energy in each phase at

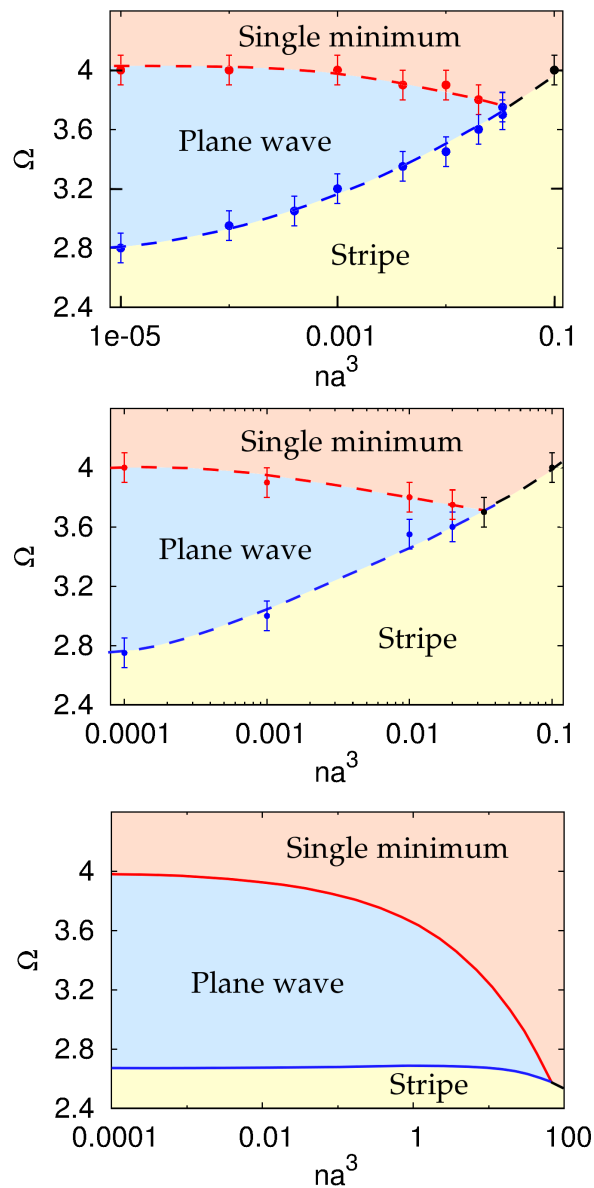


FIG. 1. Phase diagram of the many-body system with Raman Spin Orbit Coupling. The upper plot corresponds to the DTDMC diagram using the SS potential and the middle one to the LJ potential. In the lower plot, we report the mean-field phase diagram.

the mean-field level: while there is a discontinuity in this parameter between the stripe and the other two phases at the transition, the optimal momentum changes continuously from the plane wave to the single minimum phases [6, 25]. We believe that the inclusion of correlations in the DTDMC calculation does not change the nature of any of these phase transitions.

The presence of inter-atomic correlations can be seen in the pair distribution function,  $g(\vec{r}_i - \vec{r}_j)$ , which yields the probability of finding two particles with relative position vector  $\vec{r}_i - \vec{r}_j$ . For an isotropic system,  $g(\vec{r})$  depends

on  $|\vec{r}|$ , while for a non-isotropic system, as it is the case of the stripe phase, an expansion in partial waves of the form  $g(\vec{r}_i - \vec{r}_j) = \sum_{l,m} g_{l,m}(r_{ij}) Y_l^m(\theta, \phi)$  yields non-zero contributions for  $l > 0$ . Notice that, in this expression,  $\theta$  is the angle formed by  $\vec{r}$  and the  $x$ -axis, and stripes are formed along planes perpendicular to that direction. In Figure 2, we show the leading correction to the isotropic mode, for two points in the phase diagrams corresponding to the stripe and plane wave phases. Only the  $(+1, +1)$  component is reported since results for the rest of the two-body channels are analogous. The Figure depicts the  $l = 2, m = 0$  modes for the SS interaction. It should be pointed out that, for the specific type of interactions used in this work, only  $m = 0$  contributions survive. As one can see,  $g_{2,0}(r_{ij})$  is non-zero only in the stripe phase. As mentioned before, this reflects the breaking off of translational symmetry in this phase. Very similar results hold for the LJ interaction.

The presence of periodic density modulations are also seen in the static structure factor  $S(\vec{k})$ . Since in the stripe phase the  $x$ -axis is transverse to the stripe planes,  $S(k_x)$  develops a peak at a momentum proportional to the inverse of the characteristic distance separating the stripes. We show in the upper panel of Fig. 3 the static structure factor  $S(\vec{k})$  for conditions similar to the experiment of Ref. [23] ( $\gamma = 0.904$ ,  $\Omega = 0.3131$  and  $na^3 = 5 \cdot 10^{-5}$ ). The lower panel shows the same quantities for  $\Omega = 2.8$ , where the stripe modulation is much more important due to the higher value of  $\Omega$  compared to  $E_0$ . In accordance to that experiment, where reduced Raman coupling values lay in the interval  $\Omega_{\text{exp}} \in [0, 0.4]$ , we recover the stripe phase as the lowest energy state.

Finally, we characterize the superfluidity of the system in the stripe phase, where other systems have shown a non-trivial dependence along different directions [28]. In order to recreate the conditions of contrast and diluteness of Ref. [23], we set  $\gamma = 0.904$  and use gas parameters spanning the range  $na^3 \in [5 \cdot 10^{-5}, 2 \cdot 10^{-4}]$ . We mea-

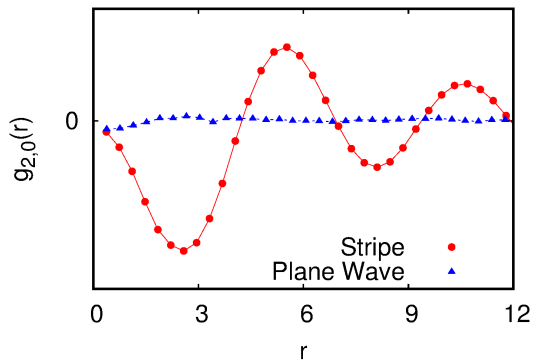


FIG. 2. Leading correction to the isotropic contribution to the pair distribution function in the  $(+1, +1)$  channel, corresponding to  $l = 2, m = 0$ , for the SS interaction.

sure the superfluid density using the zero-temperature limit of the winding number estimator [29], which is extracted from the mean squared displacement of the center of mass of the particles during imaginary time evolution. We show in Fig. 4 results for the superfluid fraction  $\rho_s^x$  in the stripe phase along the  $x$  direction, obtained from the generalization of the expression reported in Ref. [28], as a function of  $\Omega$ , and for three different values of the gas parameter,  $na^3 = 5 \cdot 10^{-5}, 1 \cdot 10^{-4}$ , and  $2 \cdot 10^{-4}$ . We see from the plot that the main parameter governing changes in  $\rho_s^x$  is  $\Omega$ , while little dependence on the specific value of the gas parameter is found. As  $\Omega$  increases, the system becomes less superfluid in the  $x$  direction. This is a direct consequence of the fact that the amplitude of the density modulation increases with  $\Omega$ , as already seen in mean-field theory [20, 24]. For large values of  $\Omega$ , exchanges of particles between different stripe planes are less favoured, and thus localization along the  $x$  axis is enhanced. In the other two directions, parallel to the stripe planes, the system remains fully superfluid ( $\rho_s^y = \rho_s^z = 1$ ), as well as in all three directions in both the plane wave and the single minimum phases, due to the lack of spatial density modulations. Notice also that, for the values of  $\Omega$  employed in the experiment of Ref. [23], the superfluid fraction  $\rho_s^x$  equals one. This, together with the periodic density modulations in the static structure factor reported in Fig. 3,

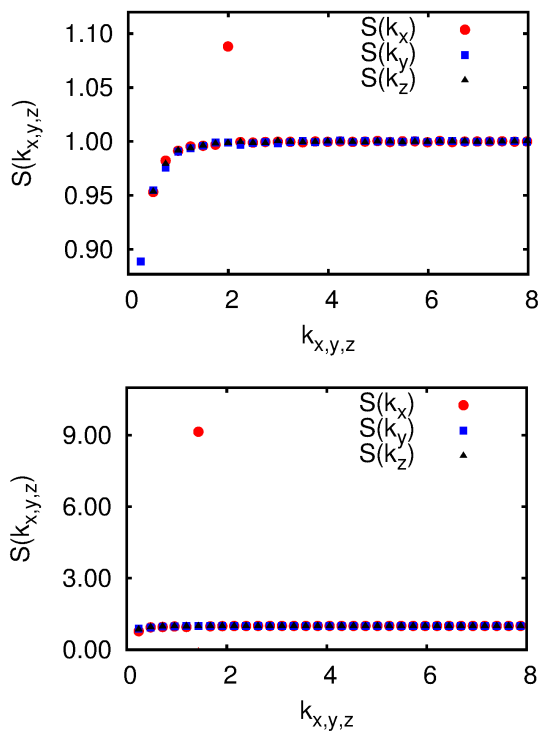


FIG. 3. Static structure factors for the SS interaction, for two different points with  $na^3 = 5 \cdot 10^{-5}$  and  $\gamma = 0.904$ , both corresponding to the stripe phase. The upper and lower panels are for  $\Omega = 0.3131$  and  $\Omega = 2.8$ , respectively.

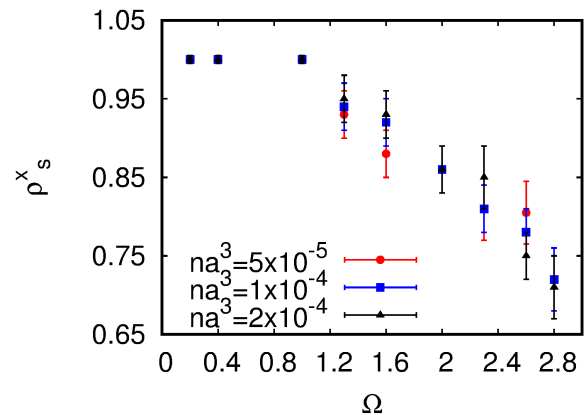


FIG. 4. Superfluid fraction for the transverse direction to the stripe planes as a function of the reduced Raman coupling for  $na^3 = 5 \cdot 10^{-5}$ ,  $\gamma = 0.904$ .

yields a quantitative indication of simultaneous spatial periodicity and superfluidity in the system. While the periodicity of stripes has been quantitatively characterized before [20, 21, 23], a quantitative proof of superfluidity, valid even beyond the mean-field regime, was still missing.

In summary, we have shown, using the DTDMC method [1, 2], that by increasing the strength of interatomic correlations in a system under Raman SOC, the region of the phase diagram covered by the stripe phase is enlarged in comparison to the prediction of mean-field theory. We have shown that this effect holds for different two-body model interactions (soft spheres and Lennard-Jones), which provide very similar results. The breaking of continuous translational symmetry in the stripe phase has been characterized by the presence of a Bragg peak in the static structure factor, and by a nonzero contribution to partial waves other than the  $l = 0$  to the pair distribution function. We have also performed DTDMC calculations in the same conditions of interaction contrast and reduced Raman coupling of the experiments of Ref. [23]. Our results confirm the observed stripes as the most energetically favorable state and quantitatively show the supersolid behavior of the stripes. We have also studied the superfluid fraction of the stripe phase as a function of the reduced Raman coupling and the gas parameter by changing the scattering length of the inter-atomic interaction. While the system is fully superfluid in the plane wave and single minimum phases, we have shown that superfluidity in the stripe phase decreases mainly as a function of the reduced Raman coupling, with little dependence on the gas parameter in the range analyzed. We hope that our work can encourage possible experimental studies of Raman SOC systems near the transition lines between the stripe and the plane wave phases, since the effects of correlations beyond the mean-field approximation can be seen even at relatively low gas parameter

values like  $na^3 = 10^{-4}$ .

This work has been supported by the MINECO (Spain) Grant No. FIS2017-84114-C2-1-P. J. Sánchez-Baena also acknowledges the FPU fellowship with reference FPU15/01805 from MECED.

---

\* juan.sanchez.baena@upc.edu

† jordi.boronat@upc.edu

‡ ferran.mazzanti@upc.edu

- [1] J. Sánchez-Baena, J. Boronat, and F. Mazzanti Phys. Rev. A **98**, 053632 (2018).
- [2] C. Melton, M. Chandler Bennett, and L. Mitas, J. Chem. Phys. **144**, 244113 (2016).
- [3] M. Z. Hasan and C. L. Kane, Rev. Mod. Phys. **82**, 3045 (2010).
- [4] M. Sato and Y. Ando, Rep. Prog. Phys. **80** 076501 (2017).
- [5] F. Wilczek, Nat. Phys. **5**, 614 (2009).
- [6] L. Zhang, X. Liu, Spin-orbit Coupling and Topological Phases for Ultracold Atoms, in *Synthetic Spin-Orbit Coupling in Cold Atoms*, edited by W. Zhang *et al.*, pp.1-87 (2018).
- [7] Y. J. Lin, K. Jiménez-García and I. B. Spielman, Nature **471**, 83 (2011).
- [8] D. Zhang, T. Gao, P. Zou, L. Kong, R. Li, X. Shen, X. Chen, S. Peng, M. Zhan, H. Pu, and K. Jiang, Phys. Rev. Lett. **122**, 110402 (2019).
- [9] P. Wang, Z.-Q. Yu, Z. Fu, J. Miao, L. Huang, S. Chai, H. Zhai, and J. Zhang, Phys. Rev. Lett. **109**, 095301 (2012).
- [10] L. W. Cheuk, A. T. Sommer, Z. Hadzibabic, T. Yefsah, W. S. Bakr, and M. W. Zwierlein, Phys. Rev. Lett. **109**, 095302 (2012).
- [11] X.-J. Liu, M. F. Borunda, X. Liu, and J. Sinova, Phys. Rev. Lett. **102**, 046402 (2009).
- [12] C. Hamner, Y. Zhang, M. A. Khamsehchi, M. J. Davis, and P. Engels, Phys. Rev. Lett. **114**, 070401 (2015).
- [13] T. M. Bersano, J. Hou, S. Mossman, V. Gokhroo, X. Luo, K. Sun, C. Zhang, and P. Engels, Phys. Rev. A **99**, 051602 (2019).
- [14] L. W. Cheuk, A. T. Sommer, Z. Hadzibabic, T. Yefsah, W. S. Bakr, and M. W. Zwierlein, Phys. Rev. Lett. **109**, 095302 (2012).
- [15] P. Wang, Z.-Q. Yu, Z. Fu, J. Miao, L. Huang, S. Chai, H. Zhai, and J. Zhang, Phys. Rev. Lett. **109**, 095301 (2012).
- [16] S. Kolkowitz, S. L. Bromley, T. Bothwell, M. L. Wall, G. E. Marti, A. P. Koller, X. Zhang, A. M. Rey, and J. Ye, Nature **542** 66-70 (2017).
- [17] B. Song, C. He, S. Zhang, E. Hajiyev, W. Huang, X.-J. Liu, and G.-B. Jo, Phys. Rev. A **94**, 061604 (2016).
- [18] L. F. Livi, G. Cappellini, M. Diem, L. Franchi, C. Clivati, M. Frittelli, F. Levi, D. Calonico, J. Catani, M. Inguscio, and L. Fallani, Phys. Rev. Lett. **117**, 220401 (2016).
- [19] N. Q. Burdick, Y. Tang, and B. L. Lev, Phys. Rev. X **6**, 031022 (2016).
- [20] Y. Li, G.I. Martone, and S. Stringari Annual Review of Cold Atoms and Molecules: pp. 201-250. (2015).
- [21] Y. Li, G. I. Martone, L. P. Pitaevskii and S. Stringari, Phys. Rev. Lett. **110**, 235302 (2013).
- [22] W. Han, G. Jazeliunas, W. Zhang, W. Liu, Phys. Rev. A **91**, 013607 (2015).
- [23] J. Li, J. Lee, W. Huang, S. Burchesky, B. Shteynas, F. Ç. Top, A. O. Jamison, and W. Ketterle, Nature **543**, 91 (2017).
- [24] A. Putra, F. Salces-Cárcoba, Y. Yue, S. Sugawa, I. B. Spielman, arXiv:1910.03613 (2019).
- [25] Y. Li, L. P. Pitaevskii, and S. Stringari Phys. Rev. Lett. **108**, 225301 (2012).
- [26] M. Casula, S. Moroni, C. Filippi, and S. Sorella, J. Chem. Phys. **132**, 154113 (2010).
- [27] X. Cui, Phys. Rev. A **85**, 022705 (2012).
- [28] R. Bombin, J. Boronat, and F. Mazzanti, Phys. Rev. Lett. **119**, 250402, (2017).
- [29] S. Zhang, N. Kawashima, J. Carlson, and J. E. Gubernatis, Phys. Rev. Lett. **74**, 1500 (1995).